*Fibers and Polymers* 2004, Vol.5, No.3, 198-203

# Morphology and Properties of Polyacrylonitrile/Single Wall Carbon Nanotube Composite Films

**Seong Hoon Kim, Byung Ghyl Min*, Sang Cheol Lee, Sung Bum Park[1], Tae Dong Lee[1], Min Park[2], and Satish Kumar[3]**

*School of Advanced Materials and System Engineering, Kumoh National Institute of Technology, Kumi 730-701, Korea*
*[1]Department of Physics, Kumoh National Institute of Technology, Kumi 730-701, Korea*
*[2]Polymer Hybrid Research Center, Korea Institute of Science and Technology, Seoul 136-791, Korea*
*[3]School of Polymer, Textile and Fiber Engineering, Georgia Institute of Technology, Atlanta, GA 30332, USA*
(Received March 22, 2004; Revised April 26, 2004; Accepted May 4, 2004)

**Abstract:** Composite films were prepared by casting the solution of polyacrylonitrile (PAN) and single wall nanotube (SWNT) in DMF subsequent to sonication. The SWNTs in the films are well dispersed as ropes with 20-30 nm thickness. Moreover, AFM surface image of the composite film displays an interwoven fibrous structure of nanotubes which may give rise to conductive passways and lead to high conductivity. The polarized Raman spectroscopy is an ideal characterization technique for identification and the orientation study of SWNT. The well-defined G-peak intensity at 1580 $cm^{-1}$ shows a dependency on the draw ratio under cross-Nicol. The degree of nanotube orientation in the drawn film was measurable from the sine curve obtained by rotating the drawn film on the plane of cross-Nicol of polarized Raman microscope. The threshold loading of SWNT for electrical conductivity in PAN is found to be lower than 1 wt% in the composite film. The electrical conductivity of the SWNT/PAN composite film decreased with increasing of draw ratio due to the collapse of the interwoven fibrous network of the nanotubes with uniaxial orientation.

**Keywords:** SWNT, Polyacrylonitrile, Nanocomposite, AFM, Raman spectroscopy

## Introduction

Carbon nanotubes have been the subject of intense research since their discovery in 1991 due to its predicted and experimentally observed excellent mechanical and electrical properties as well as highly efficient hydrogen storage properties and aspect ratio [1-8]. Recent experimental studies have shown that, besides possible improvements in the mechanical and electrical properties of polymers, the formation of nanotube/polymer composites is considered as a promising approach for an effective incorporation of nanotubes into polymer-based devices [9-15]. There has been increasing research activity on the fabrication and characterization of nanotube/polymer nanocomposites for various target applications [16-22].

However, it has been difficult to explore the full potential of these materials due to their insolubility at reasonable concentrations in common solvents. Attempts have been reported to dissolve and characterize single wall carbon nanotubes (SWNT) in various organic solvents such as dimethyl formamide (DMF) [20,21]. The physical properties of SWNT based materials, e.g., SWNT/polymer composites, SWNT fibers, and SWNT films, strongly depend upon the orientation distribution of SWNTs in the bulk sample. Therefore, for good understanding of the properties of SWNT based materials, accurate determination of the SWNT orientation is necessary [7,20-22]. SWNTs show resonance-enhanced Raman scattering effect when a visible or near infrared laser is used as the excitation source and polyacrylonitrile (PAN) as well as most other polymers do not show such a resonance effect. Therefore, the Raman spectroscopy is an ideal characterization technique for the orientation study of SWNT.

In the present study, we report morphology and orientation of SWNT in PAN films cast from DMF solution. Electrical properties of the films have also been discussed.

*Corresponding author: bgmin@kumoh.ac.kr

## Experimental

### Preparation of SWNT/PAN Solution and Composite Films

As prepared (HiPCO 86) single wall carbon nanotubes produced by the HiPCO process [24,25] were obtained from Rice University. PAN was supplied by Taekwang Ind. as a copolymer of acrylonitrile and methyl acrylate (M.W. ~ 100, 000 and AN: MA = 90:10). Dried SWNT was mixed with DMF followed by sonication for 10 hours using a bath sonicator. During the sonication process the mixtures were stirred every two hours interval with a mechanical stirrer for 30 minutes. To this dispersion PAN was added and stirred well and dissolved to get solutions containing PAN and SWNT in the ratios 99:1 and 95:5 as shown in Table 1. Films were prepared by casting the solutions on glass. The as-cast film was drawn on a hot plate up to 5 times of its original length. The films containing carbon black were also prepared at the same condition for comparison.

### Characterization

The morphology and microstructure of the SWNT were

**Table 1.** Composition of SWNT and PAN in DMF

| Component | Concentration | |
|---|---|---|
| | 1 wt% | 5 wt% |
| DMF | 22.5g | 18g |
| Filler (SWNT or carbon black) | 25 mg | 100 mg |
| PAN | 2.475 g | 1.9g |

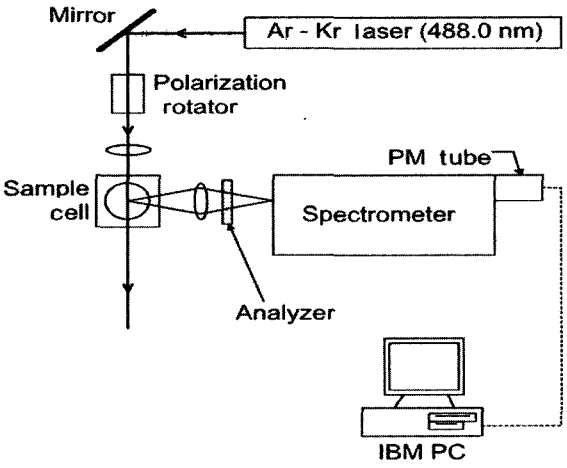


**Figure 1.** Setup for the polarized Raman spectroscopy.

characterized using atomic force microscope (AFM) and scanning electron microscopy (SEM). AFM and SEM images were obtained by using a Autoprobe in 5 (Thermo Microscope) and a field emission scanning electron microscope (FE-SEM) of Hitachi (S-4300), respectively. Cross-sections of the films for SEM were prepared by breaking in liquid nitrogen and mounted vertically on a sample stage and coated with gold before scanning. The polarized Raman spectra were excited with a $Ar^+$ ion laser (514.5 nm) and recorded using a Raman spectroscope (SpectraPro-750 of Action Research Co.). For the orientation-dependent and polarized measurements a polarizing rotator and an analyzer were set before and after a specimen on a rotating stage, respectively, at the cross-Nicol state (Figure 1). All Raman spectra were taken in backscattering configuration, with the incident and scattered light propagating perpendicular to the specimen film. Electrical resistivity of the neat PAN and PAN/SWNT composite films were measured using Kiethley 2410 sourcemeter at 10 V and 105 mA compliance.

## Results and Discussion

### Morphology of the SWNT/PAN Composite Films

The solution of the SWNT in DMF was not settling for days together, however, it could be observed that the nanotubes are still in the form of chucks. Almost all the aggregated nanotubes got dispersed very well except some hard chunks,

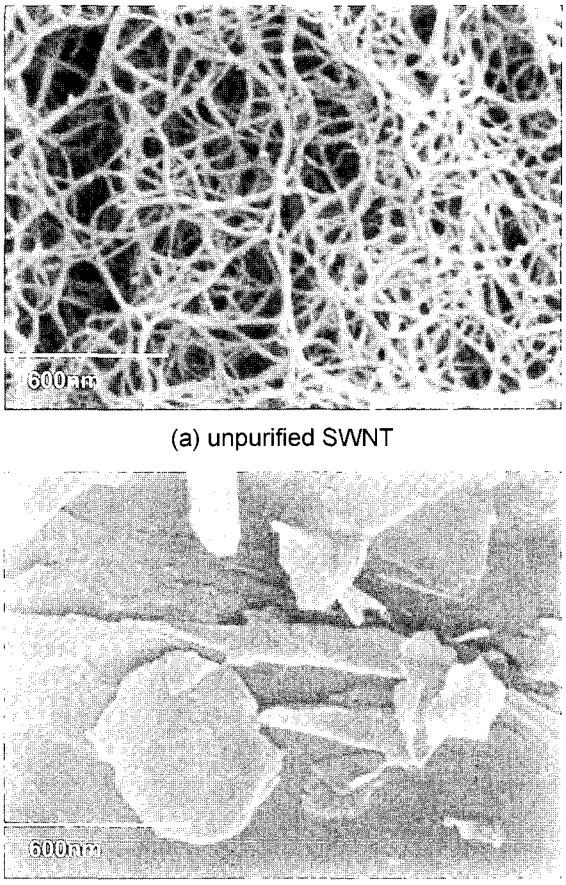


**Figure 2.** SEM micrographs of unpurified SWNT (a) and carbon black particles (b).

which might not have been swelled by the sonication process. It has been well demonstrated that Sonication of nanotubes in the presence of a solvent is a very good tool for separating the nanotube bundles and dispersing them in the solvent [26-28]. Due to the presence of PAN molecules the dispersion of nanotubes was improved and unable to coalesce back when PAN was added in the system. Carbon black used for a comparison also showed reasonable dispersibility in DMF under same condition. The films prepared by solvent casting were uniformly black at the nanotube loading.

Figure 2 shows the SEM images of the SWNT and the carbon black used. It can be seen that the SWNT bundles are very long and present as highly entangled network structure, which are responsible for the difficulty to disperse the SWNT in the polymer matrix and the relatively low solubility of the SWNT in most solvents. Figure 3 shows the typical cross-section images of SWNT/PAN and Carbon black/PAN composite films fractured in liquid nitrogen. The micrograph shows that the SWNTs were well dispersed in the composite film. They do not exist, however, as individual tubes but as ropes with 20-30 nm thickness. The typical AFM surface image of

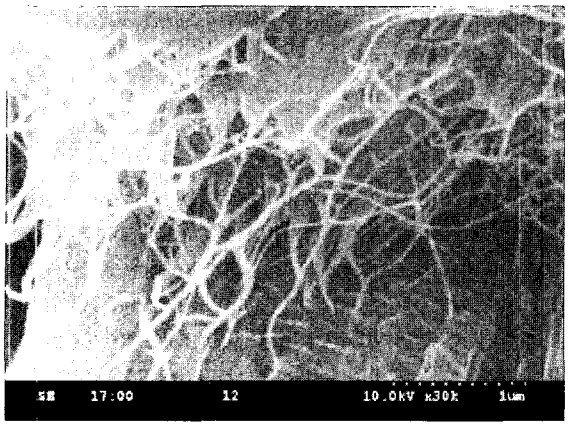


(a) PAN/SWNT (95/5)


(b) PAN/Carbon black (95/5)

**Figure 3.** Fracture images of composite films composed of PAN/SWNT (a) and PAN/carbon black (b), respectively.

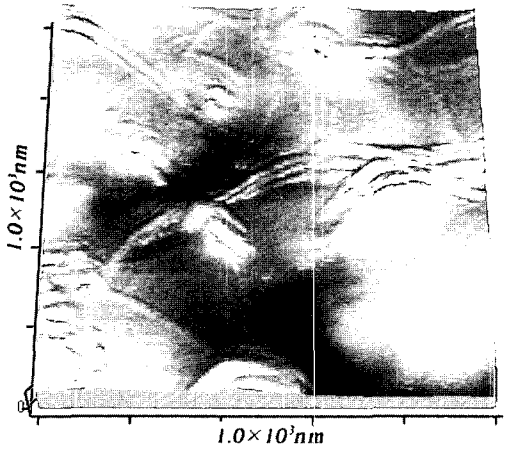


**Figure 4.** Atomic force microscopic (AFM) surface image of a SWNT/PAN (95/5) composite film showing an interwoven fibrous structure of SWNT ropes.

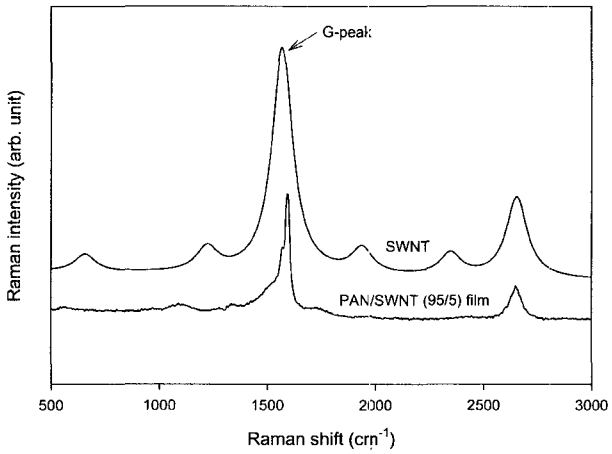


**Figure 5.** Raman spectra of SWNT and PAN/SWNT composite film with 514.5 nm excitation.

SWNT/PAN (95/5) composite film also clearly displays that the SWNTs are well dispersed in the film as individual rope or thin bundles of it, as depicted in Figure 4. Particularly, the AFM image shows that the nanotubes form an interwoven fibrous structure on the surface of the composite film. This network formation which is not seen in the film containing carbon black may give rise to conductive passways and lead to high conductivity.

Conclusively, the SWNTs could be well dispersed in the polymer matrix when the composite is prepared from solution in DMF subsequent to sonication, even though the ropes are not separated to the individual tubes.

## Orientation of SWNTs in the Composite Film by Raman Spectroscopy

Since SWNTs show resonance-enhanced Raman scattering effect when a visible or near infrared laser is used as the excitation source [29-31] and PAN as well as most other polymers do not show such a resonance effect, the Raman spectroscopy is an ideal characterization technique for the orientation study of SWNT [7,20,21,23,32-37]. In Figure 5, the spectrum of SWNT/PAN composite film is presented together with that of the neat SWNT. The well-defined G-line of the graphite at 1580 $cm^{-1}$ is observed in the composite film as well as the neat SWNT.

The G-peak intensity shows a dependency on the draw ratio of the composite film when the Raman laser passes through a polarizer or both a polarizer and an analyzer under cross-Nicol, as plotted in Figure 6. The plot shows that the orientation of the SWNT increases much amount at the initial stage of drawing followed by decreasing slope with successive drawing.

The fully drawn SWNT/PAN composite film was selected for the orientation-dependent measurements. Figure 7 displays Raman spectra with different angles, $\varphi$, between the polarization (electric field) of the incident laser light and the drawn film axis under cross-Nicol. The spectra show maximum intensity at $\varphi = 45^\circ$ and $135^\circ$ when it is rotated from 0 to $180^\circ$. This

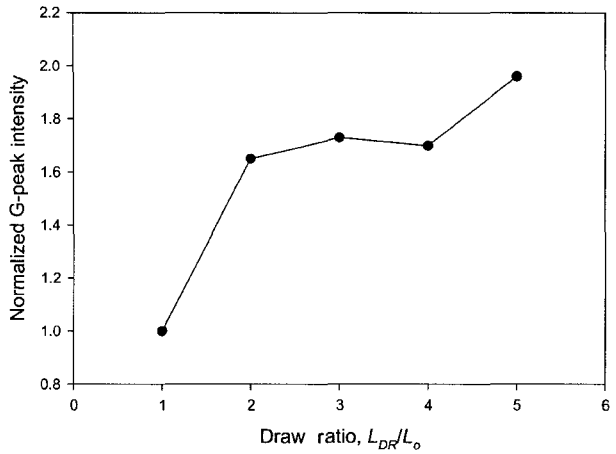


Figure 6. Dependence of G-peak intensity on draw ratio of SWNT/PAN (95/5) composite film.

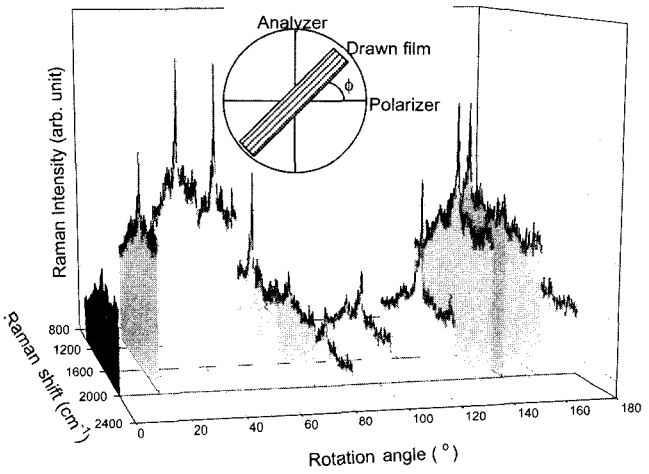


Figure 7. Raman spectra of PAN/SWNT (95/5) drawn composite film as a function of the rotation angle, $\varphi$, between the film axis and the polarization of the incident laser beam.

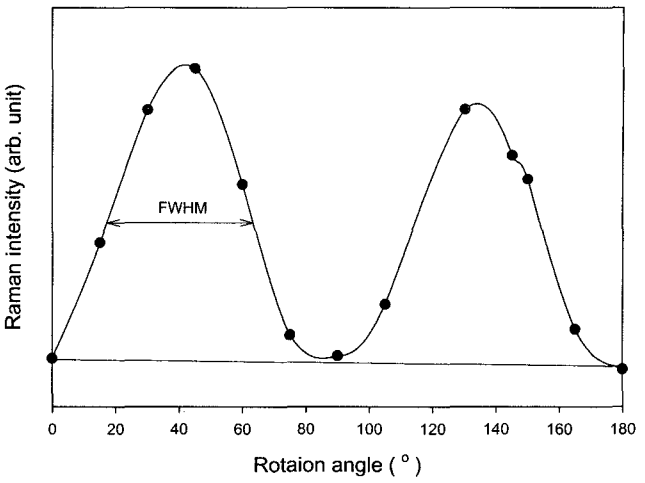


Figure 8. Raman G-peak intensity of fully drawn SWNT/PAN composite film (95/5) as a function of rotaion angle.

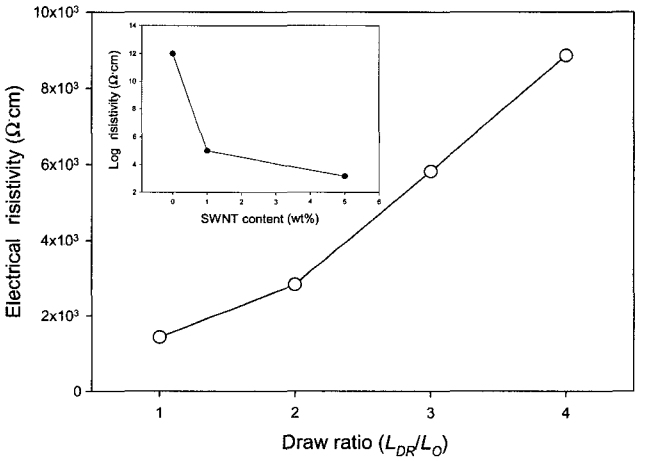


Figure 9. Dependence of electrical resistivity of SWNT/PAN composite films (95/5) on draw ratio and SWNT content (inner plot).

phenomenon is similar to that of oriented fiber or film by a polarized microscope. By plotting the G-peak intensity as a function of rotation angle as Figure 8, it is clearly seen that SWNT orients along polymer molecules by drawing the film. The full-width at half-maximum (FWHM) of the Gaussian or Lorentzian distribution function is generally taken as the measure of orientational order [30]. The FWHM value, 42 °, of the drawn composite film is relatively low compared to the value, 30 °, reported earlier in the fully drawn SWNT/PAN fiber [23]. Thus, it is concluded that polarized Raman spectroscopy is a very effective method to identify and characterize orientation of nanotubes in polymer matrix.

## Electrical Properties

As electrical properties of nanotubes make them attractive candidates for new materials, composites such that nanotubes were dispersed in a polymer matrix have been interested [38].

For a fixed intrinsic conductivity and geometry, the conductivity of the compound containing a conductive additive undergoes a classic curve as a function of loading, that is, there is a sudden transition to a conductive compound at a certain loading at which percolation occurs [39,40]. The conductivity of the PAN composite film containing 5 wt% of carbon black was out of the measurable range of the tester used, which implies that 5 wt% of carbon black is not enough for the percolation threshold loading. It is generally known that percolation occurs at around 30 % loading for carbon black. On the other hand, the composite film of PAN and SWNT exhibits a sudden drop of electrical resistivity at a SWNT loading of 1 wt%, as shown in Figure 9 (the inner plot). This means that the threshold loading of SWNT for electrical conductivity is lower than 1 wt% for the composite film. As discussed in the AFM image (Figure 4), the very effective performance of nanotube/polymer composites is originated from the interwoven

fibrous structure of nanotubes in the composite, which gives rise to conductive passways. Therefore, it is natural that the SWNT/PAN composite exhibits high conductivity compared to the carbon black/PAN composite films which do not have network structure in the matrix.

The electrical resistivity of the SWNT/PAN composite film increases with increasing of draw ratio, as depicted in Figure 9. It is considered that the reduction of conductivity with increasing of draw ratio is caused by collapse of the network conformation of the nanotubes.

## Conclusions

The SWNTs were well dispersed in the composite film not as individual tube but as rope with 20-30 nm thickness. An interwoven fibrous structure of nanotubes which is observed by AFM surface images clearly proves that the threshold loading of SWNT for electrical conductivity in PAN must be much lower than that of carbon black particle at the same content in a polymeric matrix by giving rise to effective passways for electric conductivity. The collapse of the network of the nanotubes with drawing of the film seems to be the main reason for the reduction of the conductivity with increasing of draw ratio. The Raman spectra of the drawn film show a dependency on draw ratio and give a sine curve with rotation of the drawn film on the plane of cross-Nicol, which is similar to that by polarizing microscope.

## Acknowledgement

This research was supported by Kumoh National Institute of Technology (2002-104-050).

## References

1. S. Iijima and T. Ichihashi, *Nature*, **363**, 603 (1993).
2. D. S. Bethune, C. H. Kiang, M. S. de Vries, G. Gorman, R. V. Savoy, and R. Beyers, *Nature*, **363**, 605 (1993).
3. R. Saito, G. Dresselhaus, and M. S. Dresselhaus, "Physical Properties of Carbon Nanotubes", Imperial College Press, London, 1998.
4. M. F. Yu, B. S. Files, S. Arepalli, and R. S. Ruoff, *Phys. Rev. Lett.*, **84**, 5552 (2000).
5. J. P. Lu, *Phys. Rev. Lett.*, **79**, 1297 (1997).
6. B. I. Yakobson and R. E. Smalley, *Science*, **85**, 324 (1997).
7. T. Liu, T. V. Sreekumar, S. Kumar, R. H. Hauge, and R. E. Smalley, *Carbon*, **41**, 2440 (2003).
8. A. Chatterjee and B. L. Deopura, *Fiber Polym.*, **3**(4), 134 (2002).
9. J.-E. Huang, X.-H. Li, J-C. Xu, and H-L. Li, *Carbon*, **41**, 2731 (2003).
10. M. S. P. Shaffer and A. H. Windle, *Adv. Mater.*, **11**, 937 (1999).
11. B. Z. Tang and H. Y. Xu, *Macromolecules*, **32**, 2569 (1999).
12. D. B. Romero, M. Carrard, W. A. de Heer, and L. Zuppiroli, *Adv. Mater.*, **8**, 899 (1996).
13. S. A. Curran, P. M. Ajayan, and A. Strevens, *Adv. Mater.*, **10**, 1091 (1998).
14. H. Ago, K. Petritsch, and M. S. P. Shaffer, *Adv. Mater.*, **11**, 1281 (1999).
15. A. Chatterjee and B. L. Deopura, *Fiber Polym.*, **4**(3), 102 (2003).
16. M. S. P. Shaffer and A. H. Windle, *Adv. Mater.*, **11**, 937 (1999).
17. J. Sandler, M. S. P. Shaffer, T. Prasse, W. Bauhofer, K. Schulte, and A. H. Windle, *Polymer*, **40**, 5967 (1999).
18. E. Kymakis, I. Alexandou, and G. A. J. Amaratunga, *Syn. Met.*, **127**, 59 (2002).
19. J. M. Benoit, C. Benoit, S. Lefrant, P. Bernier, and O. Chauvet, *Mater. Es. Soc. Symp. Proc.*, **706**, Z3.28.1 (2002).
20. A. R. Bhattacharyya, T. V. Sreekumar, T. Liu, S. Kumar, L. M. Ericson, R. H. Hauge, and R. E. Smalley, *Polymer*, **44**, 2373 (2003).
21. T. V. Sreekumar, T. Liu, B. G. Min, H. Guo, S. Kumar, R. H. Hauge, and R. E. Smalley, *Adv. Mater.*, **16**, 58 (2004).
22. S. Kumar, T. D. Dang, F. E. Arnold, A. R. Bhattacharyya, B. G. Min, X. Zhang, R. A. Vaia, C. Park, W. W. Adams, R. H. Hauge, R. E. Smalley, S. Ramesh, and P. A. Willis, *Macromolecules*, **35**, 9039 (2003).
23. T. Liu and S. Kumar, *Chem. Phys. Lett.*, **378**, 257 (2003).
24. P. Nikolaev, M. J. Bronikowski, R. K. Bradley, F. Rohmund, D. T. Colbert, K. A. Smith, and R. E. Smalley, *Chem. Phys. Lett.*, **313**, 91 (1999).
25. I. W. Chiang, B. E. Brinson, A. Y. Huang, P. A. Willis, M. J. Bronikowski, J. L. Margrave, R. E. Smalley, and R. H. Hauge, *J. Phys. Chem.*, **105**, 8297 (2001).
26. J. Liu, M. J. Casavant, M. Cox, D. A. Walters, P. Boul, W. Lu, A. J. Rimberg, K. A. Smith, D. T. Colbert, and R. E. Smalley, *Chem. Phys. Lett.*, **303**, 125 (1999).
27. J. M. Bonard, T. Stora, J. P. Salvetant, F. Maier, T. Stockli, C. Duschl, L. Forro, W. A. de Heer, and A. Chatelain, *Adv. Mater.*, **9**(10), 827 (1997).
28. W. Huang, Y. Lin, S. Taylor, J. Gaillard, A. M. Rao, and Y-P. Sun, *Nano Letters*, **2**(3), 231 (2002).
29. M. S. Dresselhaus and P. C. Eklund, *Adv. Phys.*, **49**, 705 (2000).
30. M. A. Pimenta, A. Marucci, S. A. Empedocles, M. G. Bawendi, E. B. Hanlon, A. M. Rao, P. C. Eklund, R. E. Smalley, G. Dresselhaus, and M. S. Dresselhaus, *Phys. Rev. B*, **58**, R16016 (1998).
31. S. D. M. Brown, A. Jorio, P. Corio, M. S. Dresselhaus, G. Dresselhaus, R. Satio, and K. Kneipp, *Phys. Rev. B*, **63**, 155411 (2001).
32. G. S. Duesberg, I. Loa, M. Burghard, K. Syassen, and S. Roth, *Phys. Rev. Lett.*, **85**(25), 5436 (2000).
33. H. H. Gommans, J. W. Alldredge, H. Tashiro, J. Park, J. Magnuson, and A. G. Rinzler, *J. Appl. Phys.*, **88**, 2509

(2000).
34. E. Anglaret, A. Righi, J. L. Sauvajol, P. Bernier, B. Vigolo, and P. Poulin, *Phys. Rev. B,* **65**, 165426 (2002).
35. J. Hwang, H. H. Gommans, A. Ugawa, H. Tashiro, R. Haggenmueller, K. I. Winey, J. E. Fischer, D. B. Tanner, and A. Rinzler, *Phys. Rev. B*, **62**, R13310 (2000).
36. R. Haggenmueller, H. H. Gommans, A. G. Rinzler, J. E. Fischer, and K. I. Winey. *Chem. Phys. Lett.,* **330**, 219 (2000).
37. J. E. Fischer, W. Zhou, J. Vavro, M. C. Llaguno, C. Guthy, R. Haggenmueller, M. J. Casavant, D. E. Walters, and R. E. Smalley, *J. Appl. Phys.*, **93**, 2157 (2003).
38. C. Stéphan, T. P. Nguyen, M. Lamy de la Chapelle, S. Lefrant, C. Journet, and P. Bernier, *Synthetic Metals*, **108**, 139 (2000).
39. D. T. Colbert, *Plastic Additives & Compounding*, Jan/Feb, 8 (2003).
40. D. Cho, Y. Choi, J. K. Park, J. Lee, B. I. Yoon, and Y. S. Lim, *Fiber Polym.*, **5**(1), 31 (2004).